Rapidly *in situ* forming hydrophobically-modified chitosan hydrogels *via* pH-responsive nanostructure transformation†

Ya-Ling Chiu,[a] Mei-Chin Chen,[a] Chun-Yu Chen,[a] Po-Wei Lee,[a] Fwu-Long Mi,[b] U-Ser Jeng,[c] Hsin-Lung Chen‡*[a] and Hsing-Wen Sung‡*[a]

Received 24th October 2008, Accepted 5th January 2009
First published as an Advance Article on the web 22nd January 2009
DOI: 10.1039/b818906d

A pH-responsive hydrogel targeted for various biomedical applications has been developed using a naturally-abundant biopolymer, chitosan, with controlled grafting of hydrophobic side chains. The rapid hydrogelation is driven by a transformation of the nanostructure of the side-chain aggregates from local micelles to interconnected nanodomains in a sponge phase due to the dominance of hydrophobic interaction near physiological pH.

Aqueous polymer solutions that can be transformed into hydrogels *in situ*, stimulated by their surrounding environment, have been proposed as injectable reservoir systems.[1] Prior to gelation, bioactive molecules or cells can be readily mixed with these solutions, thus allowing for practical pharmaceutical or tissue-engineering applications. Temperature and pH are the most common stimuli available in the human body. Temperature-sensitive hydrogels have been investigated comprehensively,[2] however, their several associated drawbacks have been reported, including diffusion of hydrogel precursors to the surrounding tissue and premature gelation inside the delivery needle/catheter.[3,4]

Here we show that a nanostructure transition triggered by the environmental pH leads to a pH-responsive biocompatible hydrogel from a naturally-abundant biopolymer, chitosan (CS). CS is a biodegradable, non-toxic and tissue compatible polysaccharide, which has been extensively used for various biomedical applications.[5] The charged state and physiochemical properties of CS are substantially influenced by its environmental pH. Considering that the pK_a of CS is *ca.* 6.0–6.5,[6] a pH-triggered hydrogelation may take place when it is brought to the physiological pH of approximately 7.4. However, at pH > 6.2, CS was found to form dissociated precipitates rather than a massive hydrogel because the aggregation of CS polymers occurred too rapidly and locally.[7]

The pH-triggered hydrogelation of CS was realized for the first time in this study by conjugating a hydrophobic palmitoyl group onto the free amine groups of CS through a convenient synthetic approach to produce a comblike associating polyelectrolyte, *N*-palmitoyl CS (NPCS, see Fig. S1 in the ESI).† Aqueous NPCS was found to form a viscous liquid-like gel at pH ≦ 6.5; here the system was called a gel because its elastic modulus (G', a measure of the material's elastic response to stress) was higher than the viscous modulus (G'', a measure of the material's viscous response to stress). A transformation from the liquid-like gel into a massive hydrogel took place at a higher pH, where transmission electron microscopy (TEM) and small angle X-ray scattering (SAXS) revealed that the aggregates of palmitoyl side chains changed from local micelles to network nanodomains in a sponge structure due to the dominance of hydrophobic interaction (Fig. 1).

The viscosity of aqueous NPCS at pH 6.5 (aqueous CS at pH 6.2) at low shear rates was investigated as a function of its degree of substitution (DS, Fig. 2). With increasing the DS, the viscosity of aqueous NPCS increased dramatically. This viscosity enhancement was due to the tendency of the hydrophobic palmitoyl side chains to form local micellar aggregates[8] that acted as the physical crosslinks between NPCS chains (*i.e.*, intermolecular crosslinks). However, up to a critical DS, the viscosity of the polymer solution (NPCS-20%) started to drop appreciably. This may be attributed to the fact that when the DS was beyond a threshold, association of the hydrophobic side chains started to have the opportunity to occur intramolecularly (*i.e.*, forming intramolecular loops).[9] The decrease of the extent of intermolecular crosslinks led to a reduction in solution viscosity as the DS was increased from 15% to 20%. Due to its highest extent of intermolecular crosslinks among all studied groups, we selected NPCS-15% for further study.

The synthesized NPCS is indeed an associating polyelectrolyte characterized by the presence of alternating charges (protonated amine groups) and hydrophobic side chains (palmitoyl groups). The balance between charge repulsion and hydrophobic interaction on NPCS chains is sensitive to the environmental pH. Fig. 3a displays the elastic modulus of aqueous NPCS-15% measured at a constant frequency of 0.1 Hz as a function of pH (see Fig. S4 in ESI for G' at other frequencies).† At pH ≦ 6.5, there was a comparative increase in G' with increasing pH. In this range of pH, although G' was larger than G'', the system flowed almost like a liquid at large shear rates due to the shear-thinning effect. When pH was raised from 6.5 to 7.0, NPCS-15% showed a drastic increase in G' by about an order of magnitude and the material was in the form of hydrogel as it responded as a solid even under large shear rates. The transition between liquid-like gel and hydrogel occurred within a narrow pH range (pH 6.5 to 7.0).

Variations in G' and G'' of aqueous NPCS-15% at pH 6.5 were found to be insignificant over the temperature range of 4 °C to 50 °C

[a]*Department of Chemical Engineering, National Tsing Hua University, Hsinchu, Taiwan, 30013, R.O.C, E-mail: hlchen@che.nth.edu.tw, hwsung@che.nthu.edu.tw; Fax: +886-3-573-8415; Tel: +886-3-572-1714*
[b]*Department of Biotechnology, Vanung University, ChungliTaoyuan, Taiwan, R.O.C*
[c]*National Synchrotron Radiation Research Center (NSRRC), Hsinchu, Taiwan, R.O.C*

† Electronic supplementary information (ESI) available: Synthesis of NPCS, rheology study information, SAXS experimental details and *in vivo* hydrogel formation information. See DOI: 10.1039/b818906d

‡ The contributions by the two collaborating parties (Dr H.W. Sung, E-mail: hwsung@che.nthu.edu.tw and Dr H.L. Chen, hlchen@che.nthu.edu.tw) are equal.

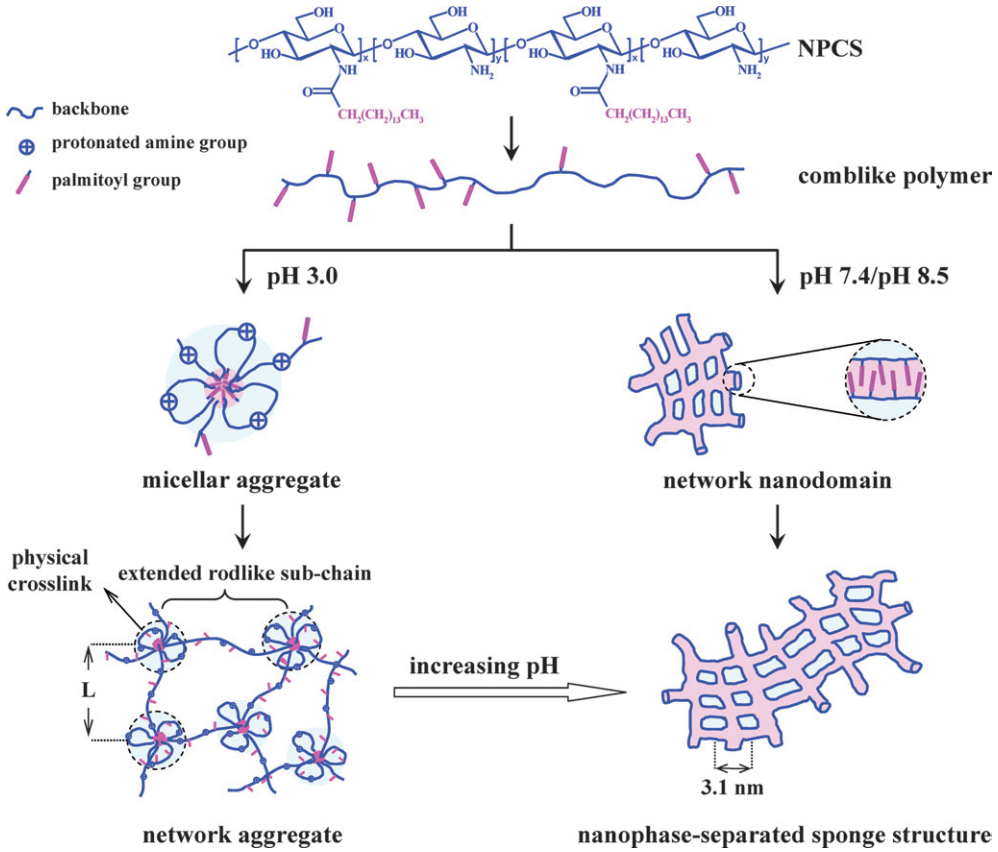

Fig. 1 Schematic illustrations of changes in structure associated with the hydrogelation of NPCS triggered by its environmental pH, revealed by small angle X-ray scattering and transmission electron microscopy. NPCS: *N*-palmitoyl chitosan with a degree of substitution of 15% (see text for details).

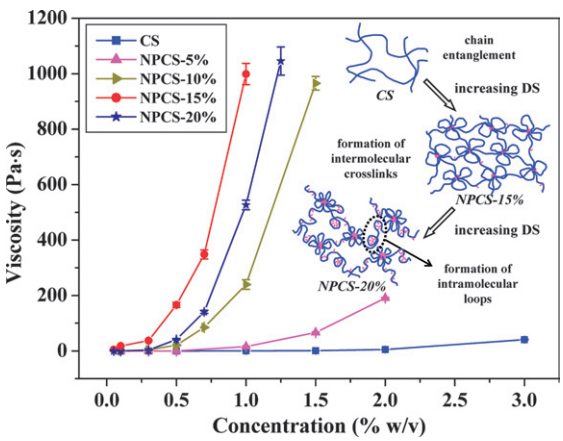

Fig. 2 Viscosity of aqueous *N*-palmitoyl chitosan (NPCS) polymers with different degrees of substitution (DS, 5%, 10%, 15% and 20%) at pH 6.5 [aqueous chitosan (CS) at pH 6.2] measured at low shear rates ($n = 5$).

(see Fig. S5 in the ESI).† This indicated that the rheological properties of aqueous NPCS-15% were not sensitive to temperature change.

To demonstrate the rapid hydrogelation triggered by pH, aqueous NPCS-15% (1% w/v) at pH 6.5 was loaded in a syringe and subsequently injected into a physiological saline solution (pH 7.4) at 37 °C through a needle. Its CS counterpart (pH 6.2) was used as a control. During injection, it was noted that both test solutions were readily squeezed through the channel of the needle. For aqueous CS after injection, local precipitates in a dissociated manner were formed in saline with time (Fig. 3b). In contrast, immediately after the injected droplet of NPCS-15% was in contact with saline, a massive hydrogel was instantly produced, thus inhibiting its diffusion in saline. Additionally, premature gelation inside the delivery vehicle could be completely avoided, since the pH of hydrogel precursors inside the needle would not be affected by their surrounding fluids. This is another significant advantage of the present pH-sensitive hydrogel over the temperature-sensitive systems.

The detailed change in supramolecular structure associated with the pH-triggered hydrogelation of NPCS-15% was examined by SAXS and TEM. At pH 3.0 where the system was in the form of liquid-like gel, the SAXS intensity exhibited a power-law dependence of q^{-1} in the high-q region ($q > 0.4$ nm^{-1}, Fig. 4a), indicating the existence of a rodlike entity in the system under larger spatial resolution.[10,11] The intensity showed an obvious increase at lower q, where the corresponding slope became *ca.* −2.7. The scattering pattern suggested that the relatively stiff NPCS-15% chains associated together to form network aggregates with a mass fractal dimension of about 2.7[11] driven by the balance between charge repulsion and hydrophobic interaction. The former, stemming from the protonated amine groups on NPCS-15%, tended to promote the molecular dispersion of polymer chains, whereas the latter caused aggregation of the hydrophobic side chains (palmitoyl groups) within an aqueous environment. Since the charge density of the CS backbone saturated to its maximum value at pH 3.0, only a limited fraction of the side

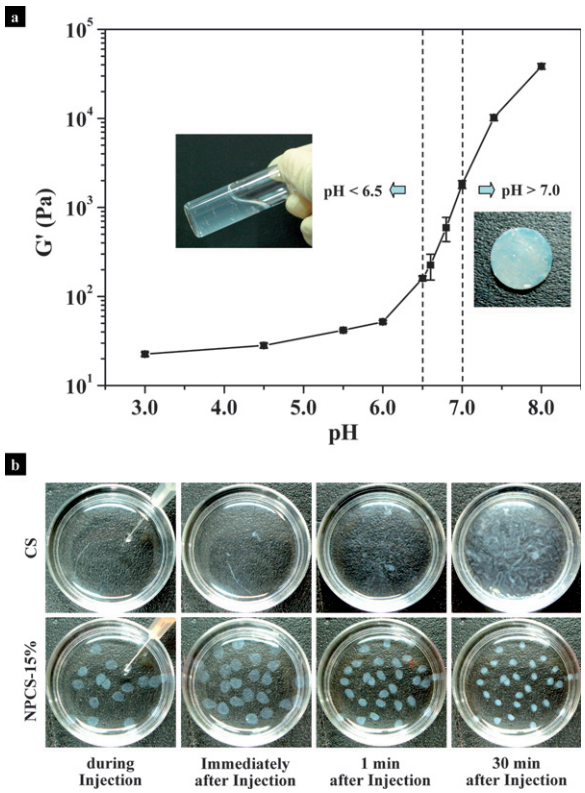

Fig. 3 (a) The elastic modulus (G') of aqueous NPCS-15% (originally at a concentration of 1% w/v) measured at a constant frequency of 0.1 Hz as a function of pH ($n = 5$); (b) Photographs of aqueous NPCS-15% at pH 6.5 [aqueous chitosan (CS) at pH 6.2] after injection through a needle into a physiological saline solution (pH 7.4) at 37 °C.

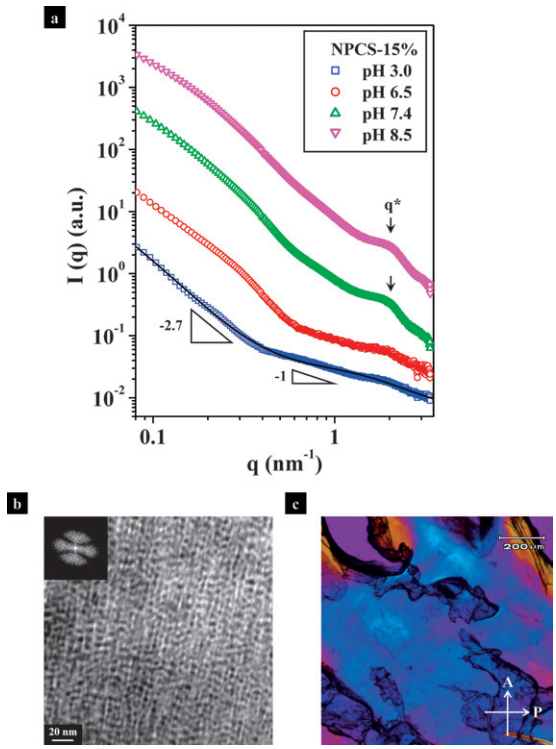

Fig. 4 (a) Small angle X-ray scattering (SAXS) profiles in log–log plots of NPCS-15% obtained at room temperature at different pH environments. The solid curve represents the result of model fitting for pH 3.0, where the model adopted was the fractal object with cylindrical building blocks. (b) A TEM micrograph and (c) a polarized optical micrograph of NPCS-15% hydrogel at pH 7.4 taken by a JEOL-2100 (HT) TEM operated at 200 kV and an Olympus BX-60 polarized optical microscope (POM), respectively. The ultrathin section (prepared by microtoming at −100 °C with a Reichert Ultracut E low-temperature sectioning system) for TEM observation was stained with OsO_4, which is a preferential staining agent for the CS backbone. The TEM micrograph revealed the formation of a sponge structure, characterized by the extensive interconnection of the nanodomains. The domains showed two preferred orientations, as manifested by the four-fold symmetry in the Fourier-transform pattern shown in the inset. The ordered sponge structure was optically anisotropic, showing the liquid crystalline birefringent texture in (c).

chains associated locally to form the physical crosslinks that tied the polymer chains to form network aggregates (Fig. 1).

Two structural levels of aggregates were hence probed by the SAXS profiles. At $q > L^{-1}$ (L = the average distance between the physical crosslinks), the intensity was dominated by the form factor of the sub-chains between the physical crosslinks, and the q^{-1} dependence of intensity attested that these sub-chains were extended resulting from the charge repulsion. At lower q where the scattering behavior was dominated by the structure at a more global level, the intensity displayed another power law of $I(q) \sim q^{-2.7}$ characterizing the fractal dimension of the network aggregates. The fitting of the observed scattering profile by the scattering function for a fractal object composed of cylindrical building blocks[12] yielded the actual fractal dimension and the correlation length (a measure for the aggregate size) of the aggregate of 2.60 and 24.7 nm, respectively (see Modeling of SAXS Profiles in the ESI).†

The SAXS pattern changed apparently when the pH was increased to 7.4 or 8.5, where the system turned into hydrogel. A peak was observed at 2 nm^{-1} following a monotonic intensity decay. At high pH, NPCS-15% lost a large fraction of charges due to deprotonation of its amine groups; therefore, the hydrophobic interaction of palmitoyl groups dominated and caused the polymer chains to aggregate significantly. In the condensed aggregates thus formed, the polar-nonpolar repulsion between the backbone and the side chains further induced a nanophase separation, and the characteristic spacing between the induced nanodomains yielded a peak in the SAXS profile.[13,14] The domain spacing (d) deduced from the SAXS peak position (q^*) *via* $d = 2\pi/q^*$ was 3.1 nm.

The real-space morphological observation of the hydrogel by TEM revealed that such a nanophase separation led to the formation of a sponge structure (Fig. 4b), characterized by the extensive interconnection of the nanodomains. These interconnected domains in the micrograph indeed showed two preferred orientations, as further manifested by the four-fold symmetry of the Fourier-transform pattern of the micrograph (the inset of Fig. 4b). The two lobes along the equator were associated with the relatively regular spacing of the vertically aligned nanodomains, while those along the meridian were due to the spacing of the horizontally aligned domains. The ordered sponge structure was optically anisotropic, showing the liquid crystalline birefringent texture[15] observed under the polarized optical microscope (Fig. 4c). Consequently, the hydrogels formed by NPCS-15% at pH 7.4 or pH 8.5 were liquid crystalline, characterized by a nanophase-separated sponge

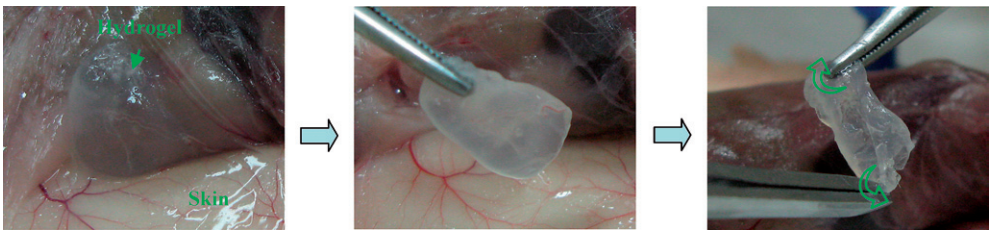

Fig. 5 Photographs of the retrieved NPCS-15% hydrogel 30 min after injection into a mouse model subcutaneously.

morphology with the characteristic domain spacing of 3.1 nm. It should be noted that the SAXS profile observed at pH 6.5 appeared to be a superposition of the two characteristic SAXS patterns seen at pH 3.0 and pH 7.4/pH 8.5, suggesting the coexistence of the two corresponding structures.

The transformation of the nanostructure associated with the pH-triggered hydrogelation of NPCS-15% was hence established based on the aforementioned SAXS and TEM results. As the pH was increased, the hydrophobic interaction of the side chains became dominant, thereby transforming the liquid-like gel composing of inter-chain network aggregates into a hydrogel, in which the polymer chains aggregated prevalently to yield the extensively interconnected nanodomains in a sponge structure.

We injected the hydrogel precursor (liquid-like gel) subcutaneously into a mouse model. Thirty minutes after injection, the mice were sacrificed. Upon retrieval, a massive hydrogel in one piece was found at the location of subcutaneous injection. The hydrogel implanted subcutaneously could be readily isolated using a pair of tweezers. After slicing longitudinally, it was observed that the center of the implant was also in the form of a hydrogel (Fig. 5).

In summary, we have developed an injectable reservoir system made of a hydrophobically-modified CS that can be rapidly transformed into hydrogel triggered by its environmental pH within a narrow range *via* a nanostructure transformation. Examined by SAXS and TEM, the hydrogel formed at physiological pH was liquid crystalline, characterized by a nanophase-separated sponge morphology. In the *in vivo* study, a massive hydrogel was found at the location of subcutaneous injection. This *in situ* forming hydrogel may enable the applications of drug delivery or tissue engineering to be performed in a minimally invasive manner.

Acknowledgements

The synchrotron X-ray scattering experiment supported by the NSRRC under Project ID 2007-1-018-2 is gratefully acknowledged. This work was supported by a grant from the National Science Council (NSC 96-2120-M-007-004), Taiwan.

Notes and references

1 K. Y. Lee and D. J. Mooney, *Chem. Rev.*, 2001, **101**, 1869.
2 B. Jeong, S. W. Kim and Y. H. Bae, *Adv. Drug Delivery Rev.*, 2002, **54**, 37.
3 H. S. Choi, K. M. Huh, T. Ooya and N. Yui, *J. Am. Chem. Soc.*, 2003, **125**, 6350.
4 J. M. Suh, S. J. Bae and B. Jeong, *Adv. Mater.*, 2005, **17**, 118.
5 M. N. V. R. Kumar, R. A. A. Muzzarelli, C. Muzzarelli, H. Sashiwa and A. J. Domb, *Chem. Rev.*, 2004, **104**, 6017.
6 M. Rinaudo, *Prog. Polym. Sci.*, 2006, **31**, 603.
7 A. Montembault, C. Viton and A. Domard, *Biomacromolecules*, 2005, **6**, 653.
8 J. Kötz, S. Kosmella and T. Beitz, *Prog. Polym. Sci.*, 2001, **26**, 1199.
9 H. Yamamoto and Y. Morishima, *Macromolecules*, 1999, **32**, 7469.
10 R. J. Roe, *Methods of X-Ray and Neutron Scattering in Polymer Science*, Oxford University Press, New York 2000, ch. 5.
11 Y. C. Li, K. B. Chen, H. L. Chen, C. S. Hsu, C. S. Tsao, J. H. Chen and S. A. Chen, *Langmuir*, 2006, **22**, 11009.
12 J. Teixeira, *J. Appl. Cryst.*, 1988, **21**, 781.
13 M. Beiner and H. Huth, *Nat. Mater.*, 2003, **2**, 595.
14 G. Floudas and P. Štepánek, *Macromolecules*, 1998, **31**, 6951.
15 G. Battaglia and A. J. Ryan, *Nat. Mater.*, 2005, **4**, 869.